Journal of the Korean Nuclear Society
Volume 29, Number 5, pp. 417~431, October 1997

〈Technical Note〉

Study on Seismic Response Characteristics of Reactor Vessel Internals and Fuel Assembly for OBE Elimination

M.J. Jhung, Y.G. Yune, J.H. Lee, and J.B. Lee
Korea Institute of Nuclear Safety
19 Kusong-dong, Yusong-gu, Taejon, 305-338, Korea

(Received February 23, 1996)

Abstract

To resolve a general argument about OBE elimination for the future nuclear power plant design, seismic responses of reactor vessel internals and fuel assembly for Ulchin nuclear power plant units 3 and 4 in Korea are investigated as an example. Dynamic analyses of the coupled internals and core are performed for the seismic excitations using the reactor vessel motions. By investigating the response relations between OBE and SSE and their response characteristics, the critical components for OBE loading are addressed. Also the fuel assembly responses are calculated using the core plate motions and their behavior is found to be insignificant for OBE elimination.

1. Background

According to ASME Boiler and Pressure Vessel Code Section Ⅲ, Division 1, Subsection NG (NG-3113) [1], each loading to which the structure may be subjected shall be classified in accordance with NCA-2142 and service limits [NCA-2142.4(b)] designated in the design specifications in such detail as will provide a complete basis for design, construction, and inspection in accordance with these rules.

The design specification may designate service limits as sets of limits which must be satisfied for all level service loadings identified in the design specifications for which these service limits are designated (NCA-2142.4). In level A service limits, the component or support may be subjected in the performance of its specified service function. In level B service limits the component or support must withstand these loadings without damage requiring repair. Level C service limits permit large deformations in areas of structural discontinuity which may necessitate the removal of the component from service for inspection or repair of damage to the component or support. Level D service limits permit gross general deformations with some consequent loss of dimensional stability and damage requiring repair, which may require removal of the component from service. Therefore, the selection of level C and D service limits shall be reviewed by the owner for compatibility with established system safety criteria (NCA-2141).

By the United States Nuclear Regulatory Commission (USNRC) Standard Review Plan (SRP) Section 3.9.3 Appendix A [2], the following loading combination shall be considered as service loadings.

(1) Level A Service Loading

Level A service loadings are derived from the normal operation loads in combination with specified system operating transient loads resulting from the normal events. Normal operating loads are defined as the sustained loads resulting from the normal

events : pressure difference, temperature and mechanical loads such as weights, loads from flow impingement or flow of reactor coolant and superimposed or reaction loads.

(2) Level B Service Loading

Level B service loadings are derived from the normal operation loads in combination with the operating basis earthquake (OBE) loads and system operating transient loads resulting from the upset events.

(3) Level C Service Loading

Level C service loadings are derived from the combination of normal operation loads and the design basis pipe break (DBPB) loads. The DBPB is defined as a postulated pipe break that results in the loss of reactor coolant at a rate less than or equal to the capability of the reactor coolant makeup system.

(4) Level D Service Loading

The following loading combination, in according with references 3 and 4, shall be considered as level D service loadings.

A. Normal operation loads
B. Branch line pipe break (BLPB) loads-Either the main steam/feedwater pipe break (MS/FWPB), or loss of coolant accident (LOCA) loads whichever are larger
C. Safe shutdown earthquake (SSE) loads

LOCA is defined as the loss of coolant at a rate in excess of the reactor coolant normal makeup rate, from breaks in the reactor coolant pressure boundary inside primary containment up to, and including, a break equivalent in size to the largest remaining primary branch line not eliminated by leak before break (LBB) criteria.

For the service loadings, two earthquakes (OBE and SSE) are included in level B and level D loadings, respectively. OBE is defined in section Ⅲ (d) of Appendix A to 10 CFR Part 100 [3] as that earthquake which, considering the regional and local geology and seismology and specific characteristics of local subsurface material, could reasonably be expected to affect the plant site during the operating life of the plant. It is that earthquake which produces the vibratory ground motion for which those features of the nuclear power plant, necessary for continued operation without undue risk to the health and safety of the public, are designed to remain functional. SSE is defined in section Ⅲ (c) of Appendix A to 10 CFR Part 100 as that earthquake which is based upon an evaluation of the maximum earthquake potential considering the regional and local geology and seismology and specific characteristics of local subsurface material. It is the earthquake which produces the maximum vibratory ground motion for which certain structures, systems, and components are designed to remain functional. These structures, systems, and components are those necessary to assure :

(1) The integrity of the reactor coolant pressure boundary.
(2) The capability to shut down the reactor and maintain it in a safe shutdown condition, or
(3) The capability to prevent or mitigate the consequences of accidents which could result in potential offsite exposures comparable to the guideline.

Also the postulated pipe breaks are included in the level C and D service loadings since the earliest plants. The first reason for postulating a break was to calculate the design basis containment pressure. The next reason was to consider the effect of the loss of coolant in the design basis for the emergency core cooling systems. These considerations are relatively independent of the mechanical details at a given postulated pipe break location, and governed primarily by thermal-hydraulic system parameters.

More recent considerations of the mechanical and structural consequences of postulated pipe ruptures, including thrust forces on the piping, jet impingement on the surrounding compartment, internal hydraulic loads and sub-compartment pressurization, require more precise definition of the mechanical details at a postulated pipe break location.

It is emphasized that catastrophic pipe breaks which result in double ended guillotine break (DEGB) are highly improbable, but are postulated to establish a

highly conservative design basis. The stringent quality assurance provisions imposed on the design, the quality control provisions in the manufacturing process [1] and the inservice inspection procedures employed on site [4] provide a very high level of assurance that catastrophic pipe breaks will not occur in nuclear class 1 piping [5]. To balance these considerations against the consequences of a postulated accident, even though remote, the USNRC and the nuclear industry standards groups have established a reasonable yet conservative pipe break philosophy. The basic philosophy predicts that the location of a pipe break should be postulated at the point of the highest stress range or cumulative usage factor.

Prior to 1983, General Design Criteria 4 (GDC-4) of 10 CFR 50 Appendix A [6] required plant designers to consider the dynamic effects of postulated main coolant loop (MCL) breaks as well as tributary pipe breaks in mechanical design. Pipe break requirements for mechanical design have since evolved to a more reasonable technical basis than the full double ended guillotine break originally required by GDC-4. Probabilistic and deterministic studies performed in the 1980's under USNRC sponsorship demonstrated that the probability of leakage, especially a DEGB is very low and that flaws in pipes can be detected before the flaws can grow to a critical length from which a DEGB could occur. The deterministic studies utilized a fracture mechanics technology now termed leak-before-break (LBB). The development of LBB methodology culminated in NUREG-1061 Volume 3 [5], in which the USNRC established guidelines for application of LBB.

In parallel, regulatory requirements evolved to the 1986 "limited scope" rule of GDC-4, allowing the application of LBB techniques to demonstrate that consideration of MCL breaks in pressurized water reactors could be eliminated, and to the 1987

Table 1. Primary side pipe breaks postulated for service level D loadings

Unit	Pipe break	Location	Break type	Flow area[1]
Palo Verde	Hot leg	RV terminal end	Guillotine	100
		SG terminal end	Guillotine	600
	Discharge leg	RV terminal end	Guillotine	350
		Pump terminal end	Guillotine	480
	Suction leg	Pump terminal end	Guillotine	430
		Pump elbow	Slot	532
		SG elbow	Slot	532
		SG terminal end	Guillotine	592
YGN 3&4	16″ shutdown cooling line	115.4″ from RV outlet nozzle	Guillotine	129
	12″ surge line	115.4″ from RV outlet nozzle	Slot, guillotine	97
	3″ PZR spray line	RV inlet nozzle	Guillotine	5
	14″ safety injection line	RV inlet nozzle	Guillotine	117
UCN 3&4	6″ safety valve nozzle	159.5″ from RV nozzle safe end	Guillotine	21
	3″ long term safety injection line	154.2″ from RV nozzle safe end	Guillotine	5
	3″ PZR spray line	194.4″ from RV nozzle safe end	Guillotine	5
	4″ PZR spray line intermediate break	194.4″ from RV nozzle safe end	Slot, guillotine	5

[1]Unit = in^2

"broad scope" rule of GDC-4, allowing the LBB approach to extend, when justified, to all high energy piping systems in nuclear power plants. The USNRC SRP Section 3.6.3 implements the "broad scope" rule of GDC-4 and endorses the LBB methodology of NUREG-1061 Volume 3 [5].

MCL breaks were the design bases for the Palo Verde unit 1 which was designed in the late seventies as shown in Table 1. In 1983, Combustion Engineering performed LBB evaluation for the MCL and submitted a Standard Safety Analysis Report (CESSAR), which was later accepted by the USNRC. MCL pipe breaks were not design basis for the Yonggwang nuclear power plant units (YGN) 3 and 4 in Korea because those piping system is virtually the same as CESSAR plants'. Instead two inlet (14 inch safety injection nozzle and 3 inch pressurizer spray line nozzle) and two outlet (16 inch shutdown cooling nozzle and 12 inch surge line nozzle) breaks in the primary side were postulated for the branch line pipe breaks. Of these four breaks, LBB evaluation was performed for the piping system with a diameter of 10 inches or over. For the Ulchin nuclear power plant units (UCN) 3 and 4 in Korea, 4 primary side pipe breaks with less than 10 inches (3 inch pressurizer spray line break, 4 inch pressurizer spray line intermediate break, 6 inch pressurizer safety valve inlet nozzle break and 3 inch long term safety injection line break) are postulated and their response on the reactor vessel internals (RVI) is considered as level C or D service loadings.

For component elastic analysis, limits of stress intensities for each service level are shown in Table 2. The allowables for service levels C and D are not changed even though the loads decreased much because of the decrease of the pipe break loads due to the application of LBB concept. This made it possible to anticipate that the loading condition controlling the design be changed from level D loading to level B loading. Tables 3 and 4 show the safety margin for YGN 3 and Palo Verde 1 RVI components, respectively [7, 8]. It is clear that level B service loading rather than level D is controlling the design of YGN 3 reactor internals, which means that OBE is controlling the RVI component designs.

In this respect, NRC staff requested the Commission's approval to decouple the level of the OBE ground motion from that of the SSE in SECY-90-016 [9]. The Commission approved the staff's position in its staff requirements memorandum (SRM) of June 26, 1990. The elimination of the OBE from design was requested by the Electric Power Research Institute and also recommended by the Advisory Committee on Reactor Safeguards in its letter of April 26, 1990. In SECY-93-087 [10], the staff further requested that the Commission approve eliminating the OBE from the design of all structures, systems, and components in design of both evolutionary and passive advanced reactors.

To resolve a general argument about OBE elimination for the future nuclear power plant design, seismic responses of reactor vessel internals and fuel assembly for Ulchin nuclear power plant units 3 and 4 in Korea are investigated. Dynamic analyses of the coupled internals and core are performed for the seismic excitations using the reactor vessel motions. The

Table 2. Limits of Stress Intensities for Each Service Level

Service Level	Primary stresses		Section III, Division 1[1]
A	$P_m < S_m$	$P_m + P_b < 1.5S_m$	NG, Fig.NG-3221-1
B	$P_m < S_m$	$P_m + P_b < 1.5S_m$	NG, Fig.NG-3221-1
C	$P_m < 1.5S_m$	$P_m + P_b < 2.25S_m$	NG, Fig.NG-3224-1
D	$P_m < 2.4S_m$	$P_m + P_b < 3.6S_m$	Appendix F, F-1440

[1] Ref.1

Table 3. Safety Margin of RVI Components for YGN Unit 3

Component	Stress Type	Margin (%)[1] for Service Level		
		A&B	C[2]	D
CSB Upper Flange	P_m	72	–	85
	P_m+P_b	37	–	59
CSB Lower Flange	P_m	39	–	61
	P_m+P_b	35	–	58
Lower Support Structure	P_m	7	–	52
	P_m+P_b	10	–	29
UGS Upper Flange	P_m	67	–	83
	P_m+P_b	54	–	78
UGS Lower Flange	P_m	59	–	82
	P_m+P_b	63	–	84
Tube Sheet Assembly	P_m	64	–	76
	P_m+P_b	3	–	41

[1] Margin (%) = (1 − calculated/allowable) × 100.

[2] Not checked for Level C loadings because the Level C requirements are not controlling for the core support structure loads.

Table 4. Safety Margin of RVI Components for Palo Verde Nuclear Power Plant Unit 1

Component	Stress Type	Margin (%)[1] for Service Level		
		A&B	C[2]	D
CSB Upper Flange	P_m	78	–	76
	P_m+P_b	60	–	35
CSB Lower Flange	P_m	86	–	61
	P_m+P_b	67	–	46
Lower Support Structure	P_m	42	–	42
	P_m+P_b	39	–	7
UGS Upper Flange	P_m	52	–	21
	P_m+P_b	49	–	23
UGS Lower Flange	P_m	93	–	71
	P_m+P_b	72	–	9
Tube Sheet Assembly	P_m	87	–	91
	P_m+P_b	37	–	32

[1] Margin(%) = (1-calculated/allowable) × 100.

[2] Not checked for Level C loadings.

response relations between OBE and SSE and their response characteristics are investigated. Also the fuel assembly responses are calculated using the core plate motions and their behavior is investigated.

2. Dynamic Response of Reactor Vessel Internals

2.1. Model Development

The mathematical model of the internals consists

of lumped masses and elastic beam elements to represent the beam-like behavior of the internals, and nonlinear elements to simulate the effects of gaps between components. Typical component gaps represented by nonlinear elements in the horizontal direction are the core support barrel, pressure vessel snubber gap and core shroud guide lug gap. The gaps between the core shroud and core support barrel or the core support plate and core support barrel are sufficiently large that no contacting occurs. For the vertical direction, the gap between CEA (control element assembly) guide tube and upper end fitting of the fuel assembly is represented by nonlinear element.

At appropriate locations within the internals and core, nodes are chosen to lump the weights of the structure. The criterion for choosing the number and location of mass points is to provide for accurate representation of the dynamically significant modes of vibration for each of the components. For the beam element connecting two nodes in the horizontal model, properties are calculated for moment of inertia, cross-sectional area, effective shear area, stiffness and length. For the vertical stiffness, a well known formula $K = AE/L$ is used where K, A, E and L are axial stiffness (lb/in), cross-sectional area (in^2), Young's modulus (psi) and length of segment (in), respectively.

Stiffnesses for the complex structures such as UGS and CSB flanges, CSB snubber, hold-down ring and CEA guide tubes are determined by finite element analyses. Unit deflections and rotations are applied and the resulting reaction forces are calculated. These results are then used to derive the equivalent member properties for the structure.

The CSB upper region is modeled to account for the possible interactions between the CSB upper flange, UGS upper flange, hold-down ring and the reactor vessel ledge using the nonlinear, hysteresis and friction elements. But if justified by analysis, it can be modeled as one mass point. A dynamically equivalent representation of the CEA shroud is included in the horizontal model. This representation is based on the frequency analysis of a detailed finite element model [11, 12, 13]. Typical coupled internals and core models in the horizontal and vertical directions are shown

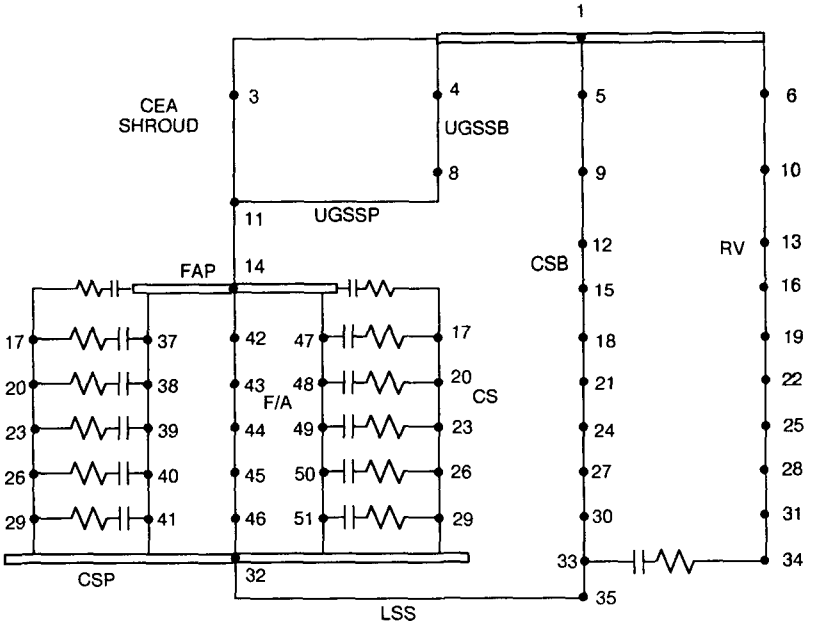

Fig. 1. Lumped Mass Model of Coupled Internals and Core in the Horizontal Direction

in Figures 1 and 2. The actual arrangement and detail in the model may vary with the function of plant design, and the magnitude and nature of the excitation.

2.2. Analysis

Using the lumped mass model developed above, the time history analyses are performed for the earthquake motions of design for Ulchin nuclear power plant units 3 and 4 which are reference plants for Korean standard nuclear power plant. The design basis earthquake has maximum free field horizontal ground accelerations at the foundation level of 0.2g for the SSE and 0.1g for the OBE. The maximum vertical ground accelerations are 0.13g and 0.067g

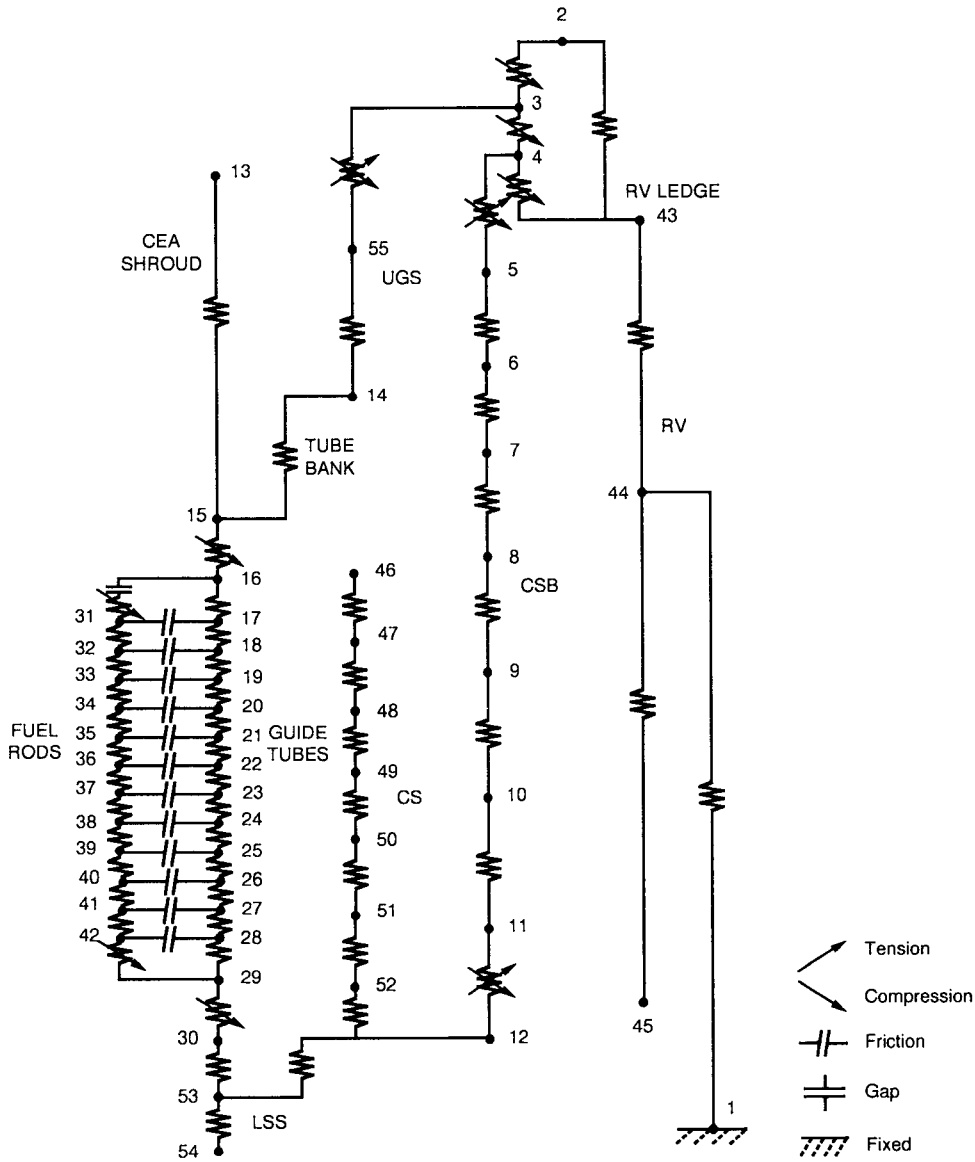

Fig. 2. Lumped Mass Model of Coupled Internals and Core in the Vertical Direction

for the SSE and OBE, respectively.

2.2.1. Input Excitations

The forcing function to the horizontal model consists of acceleration time histories at the RV flange and snubber elevations determined from the reactor coolant system (RCS) analysis. The reactor vessel is so stiff comparing with internals components that its local effect is negligible. Therefore, only translational accelerations on the RV between the flange and snubbers are computed by linear interpolation and are input into the model. These translational accelerations along the vessel are required for the calculation of hydrodynamic forces between CSB and RV annulus. The input excitations to the vertical model consist of RV flange motion only which is determined from the reactor coolant system analysis.

The acceleration time histories of RV flange and its corresponding spectra are shown in Figures 3 and 4, respectively. The peak values of input motions are shown in Tables 5 and 6. The maximum accelerations in the east-west direction for the SSE are 233.2 in/sec^2 (0.604g) at 6.043 seconds and 144.9 in/sec^2 (0.375g) at 11.803 seconds for the RV flange and snubber elevations, respectively. For OBE, the maximum values are 141.8 in/sec^2 (0.367g) at 6.045 seconds and 83.6 in/sec^2 (0.216g) at 6.043 seconds for the RV flange and snubber elevations, respectively. An amplification factor of zero period acceleration (ZPA) values from RCS basemat to RV flange is in the range of 2.1 to 3.1 in the horizontal direction and 1.5 in the vertical direction (Table 7). The corresponding values from design basis earthquake (DBE) to RCS basemat are 1.2 and 1.5. This indicates that RVI is more amplified than RCS components which

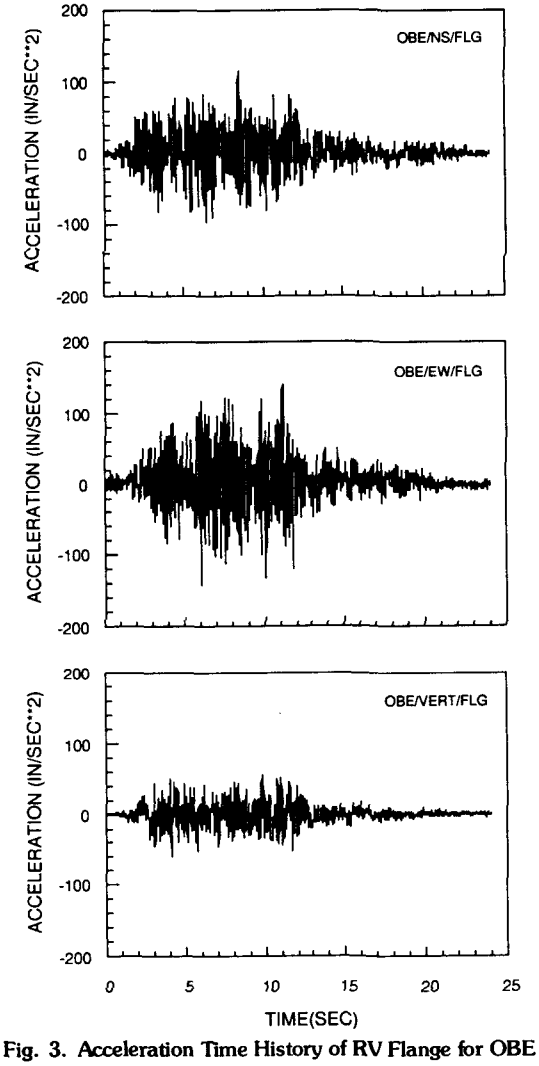

Fig. 3. Acceleration Time History of RV Flange for OBE

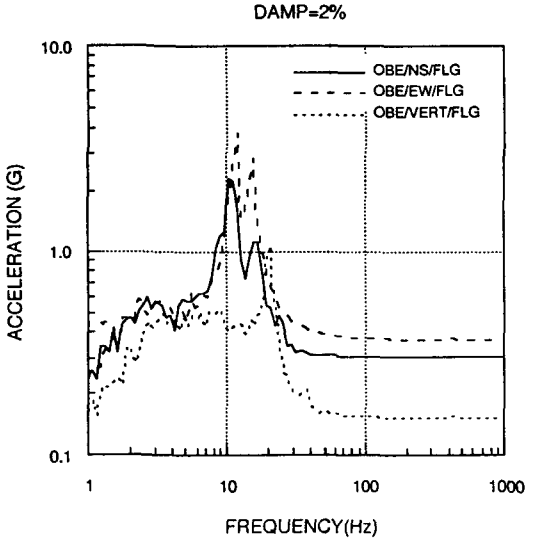

Fig. 4. Response Spectra of RV Flange for OBE

Table 5. Peak Values of Input Motion for RVI Analysis

Earthquake	Dir.[1]	RV flange				RV snubber			
		acce. (in/sec^2)	time (sec)	spectra (g)	freq. (Hz)	acce. (in/sec^2)	time (sec)	spectra (g)	freq. (Hz)
OBE	N-S	116.4	8.485	2.278	10.23	52.1	7.088	0.554	2.68
	E-W	141.8	6.045	3.749	11.78	83.6	6.043	1.550	15.62
	Vert.	58.6	4.095	1.058	20.71	–	–	–	–
SSE	N-S	197.0	8.485	2.396	10.23	102.6	7.088	0.835	3.09
	E-W	233.2	6.043	3.507	11.78	144.9	11.803	1.656	14.56
	Vert.	111.3	9.845	1.251	20.71	–	–	–	–
Ratio(%)									
OBE/SSE	N-S	59.1		95.1		50.8		66.3	
	E-W	60.8		106.9		57.7		93.6	
	Vert.	52.7		84.6		–		–	

[1] N-S: north-south direction, E-W: east-west direction, Vert.: vertical direction.

Table 6. ZPA(g) Values of Input Motions for RCS, RVI and Core Analysis

Earthquake	Direction	DBE[1]	RCS	RV		CORE[2]	
			basemat	flange	snubber	FAP (UEF)	CSP (LEF)
OBE	N-S	0.1	0.119	0.301	0.135	0.960	0.366
	E-W	0.1	0.119	0.367	0.216	1.401	0.475
	Vert.	0.067	0.099	0.152	–	0.215	0.207
SSE	N-S	0.2	0.238	0.510	0.266	1.532	1.720
	E-W	0.2	0.238	0.604	0.375	3.201	1.298
	Vert.	0.133	0.197	0.288	–	0.390	0.377
Ratio(%)							
OBE/SSE	N-S	50.0	50.0	59.1	50.8	62.7	21.3
	E-W	50.0	50.0	60.8	57.7	43.8	36.6
	Vert.	50.0	50.0	52.7	–	55.1	54.9

[1] DBE = Design basis earthquake.

[2] For horizontal direction ZPAs of FAP and CSP are tabulated and for vertical direction ZPAs of UEF and LEF are tabulated.

Table 7. Amplification Factor of ZPA Values for AE, RCS and RVI Analysis

Earthquake	Dir.	AE	RCS	RVI
		DBE→RCS basemat	RCS basemat→RV flg.	RV flg.→core plt.[1]
OBE	N-S	1.2	2.5	3.2
	E-W	1.2	3.1	3.8
	Vert.	1.5	1.5	1.4
SSE	N-S	1.2	2.1	3.4
	E-W	1.2	2.5	5.3
	Vert.	1.5	1.5	1.4

[1] For vertical direction, end fittings of fuel assembly are used.

has more supporting system to absorb the earthquake motion. In this respect, a novel idea for supporting system in the RVI components is necessary, which is assumed to be almost impossible due to the function of providing a flow path.

2.2.2. Dynamic Response

The response of the reactor vessel internals is computed by the SHOCK code [14], which solves for the response of the structures represented by lumped mass and spring systems under a variety of loadings. This is done by numerically solving the differential equations of motion for an N degree of freedom system using the Runge-Kutta-Gill technique. The equation of motion can represent an axially responding system or a horizontally responding system i.e., an axial motion or a coupled horizontal and rotational motion. The code is designed to handle a large number of options for describing load environments and includes such transient conditions as time-dependent forces and moments, initial displacements and rotations, and initial velocities. Options are also available for describing steady-state loads, preloads, accelerations, gaps, nonlinear elements, hydrodynamic mass, viscous damping, friction, and hysteresis.

Equilibrium conditions, prior to the application of the vertical dynamic transient conditions, are established by determining the static displacements associated with the weight of the internals and core in water, preloads and the core drag steady state forces. These calculated static displacements are used as the initial conditions. Without these, some of the masses would be subjected to large accelerations because of the resulting force unbalance.

2.3. Results and Discussion

The results of analysis consist of shear, moment and axial force of each component which will be used for design loads, and motions for core shroud, fuel alignment plate (FAP) and core support plate (CSP) which will be used for the detailed core analysis. Also, the response spectra at several locations of

Table 8. Load Summary for RVI Components

Component	OBE				
	N-S		E-W		Vertical
	shear(lb)	moment(in-lb)	shear	moment	axial force(lb)
CSB Upper Flange	.1845E6	.3311E8	.3055E6	.3134E8	93000
CSB Lower Flange	.5745E5	.4329E7	.1095E6	.7856E7	73000
LSS	.4919E5	.4311E7	.9401E5	.7788E7	58000
UGS Upper Flange	.1720E6	.1422E8	.3017E6	.2520E8	20000
UGS Lower Flange	.5672E5	.2261E7	.7669E5	.2373E7	17000
Tube Sheet Assembly	.3341E5	.2162E7	.3788E5	.2462E7	14000
Component	SSE				
	N-S		E-W		Vertical
	shear	moment	shear	moment	axial force
CSB Upper Flange	.4063E6	.4332E8	.7000E6	.5049E8	171000
CSB Lower Flange	.2023E6	.1041E8	.2684E6	.1851E8	133000
LSS	.1477E6	.1027E8	.2098E6	.1830E8	105000
UGS Upper Flange	.2384E6	.1872E8	.5767E6	.4204E8	39000
UGS Lower Flange	.1016E6	.3799E7	.1429E6	.4737E7	32000
Tube Sheet Assembly	.6032E5	.4028E7	.8211E5	.5091E7	28000

[1] Unit: shear (lb), moment(in-lb), axial force(lb)

Table 9. Ratio (%) of OBE/SSE Loads for RVI Components

Component	N-S		E-W		Vertical
	shear	mom.	shear	mom.	force
CSB Upper Flange	45.4	76.4	43.6	62.1	54.4
CSB Lower Flange	28.4	41.6	40.8	42.4	54.9
LSS	33.3	42.0	44.8	42.6	55.2
UGS Upper Flange	72.1	76.0	52.3	59.9	51.3
UGS Lower Flange	55.8	59.5	53.7	50.1	53.1
Tube Sheet Assembly	55.4	53.7	46.1	48.4	50.0

the reactor vessel internals are generated for the ensuing stress analysis to verify the structural integrity of the core support structures.

The response loads of core support structures are summarized in Table 8. It is found that upper flanges of CSB and UGS are most severe response region in all three directions, which is anticipated that they are so near to the RV ledge region where the earthquake motion is directly applied. The response ratio of OBE to SSE is also shown in Table 9. The most response ratio obtained is 72.1 % in UGS upper flange for shear, 76.4% in CSB upper flange for moment and 55.2% in LSS for axial force. The response ratio ranges in 28.4% to 76.4% for north-south direction and 40.8% to 59.9% for east-west direction. UGS flanges show high response ratio compared to other components. For the vertical direction, the ratio is in the range of 50.0% to 55.2%, which corresponds to the ratio of ZPA value (52.7%) of RV flange motion very well. This is possible because major frequencies in the vertical direction are high and the ZPA is obtained around those frequencies. Generally OBE responses for UGS upper flange and CSB upper flange are higher than half of SSE responses, but CSB lower flange and LSS responses are lower than half of SSE responses.

For the subsequent detailed core analysis the response spectra for the fuel alignment plate and core support plate are investigated. The ZPA values for FAP are 1.401g and 3.201g in the east-west direction for OBE and SSE, respectively (Table 6). An

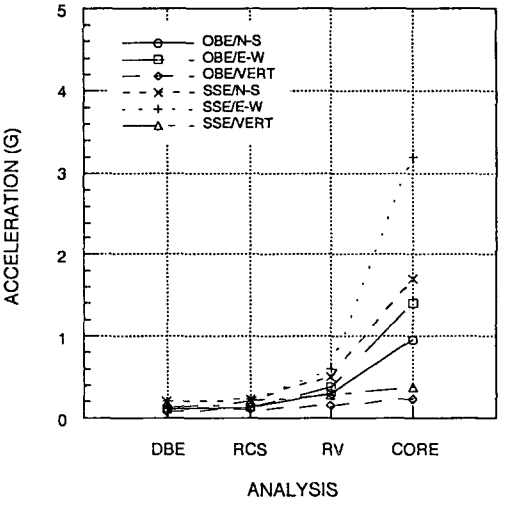

Fig. 5. Zero Period Accelerations of DBE, RCS, RVI and Core Analysis

amplification factor of ZPA values from RV flange to FAP is in the range of 3.2 to 5.3 as shown in Table 7 and Figure 5. But the spectra values between 1 Hz and 10 Hz are not much amplified as shown in spectra plot and therefore fuel assembly is not anticipated to produce big response because the major fuel assembly modes fall between 1 Hz and 10 Hz [15].

3. Dynamic Response of Fuel Assembly

3.1. Model Development

In the detailed horizontal core model, the fuel assemblies are modeled as uniform beams. Lumped

masses are included at spacer grid locations to represent the significant modes of vibration of the fuel and to account for possible spacer grid impacting. Nonlinear spring couplings are used to simulate the gaps in the core. Each spacer grid is characterized by the dual load path model which represents the load paths associated with both one-sided and through-grid impacts. One-sided loads are the loads experienced by one side of a grid when it impacts on another grid or the core shroud. Through-grid loads are the loads developed through grid loadings on a spacer grid.

The fuel analytical model was constructed by calculating nodal properties for corresponding locations based on the weight distribution data. The dynamic characteristics of the fuel bundle including natural frequency and damping were also determined from the test data. The static model of the fuel bundle was modified to include dynamic effects by adjusting the bundle stiffness to obtain the proper natural frequency and prescribing the damping as a percentage of critical damping.

Hydrodynamic (diagonal coupling coefficients) mass was added to the structural mass to obtain the proper natural frequency in water. The off-diagonal coupling terms are not considered in the core model, that is, hydraulic coupling between the fuel assemblies is neglected. This was justified by water loop tests [16], which indicate that the natural frequency drop can be accounted for by added masses corresponding to the displaced liquid, meaning that a fuel assembly in a channel does not behave in a significantly different manner as a fuel assembly in an infinite fluid. Physically this means that without a wrapper tube, the fluid can flow from one side of the assembly to the other, across the fuel assembly rather than around it.

The spacer grid model was developed considering impacting of adjacent fuel assemblies or peripheral assemblies and the core shroud. If two fuel assemblies hit another or if one assembly strikes the core shroud, then the spacer grids are loaded on only one force. This type of impact has been called a one-sided impact. The second impact type is called a through-grid impact because the impact force is applied simultaneously to opposite faces of the spacer grid. For example, a through-grid impact occurs when one fuel assembly is lying against the core shroud and a second assembly hits it [17]. Therefore, the spacer grid model separates out through-grid and one-sided load paths. The pluck vibration, pluck impact, spacer grid compression, and spacer grid section drop tests provide data used in determining the spacer grid impacting parameters.

3.2. Analysis

The detailed horizontal core model is developed for the time history analysis for the seismic excitations, and dynamic response is determined using the core plate motions from the coupled internals and core analysis. The vertical response is obtained in the coupled internals and core model and therefore separate analysis is not required.

3.2.1. Input Excitations

The input excitations to the detailed core model consist of the translational and angular motions of the core plates and the translational motion of the core shroud. The core shroud is so stiff comparing with fuel assembly that its local effect is negligible. Therefore, only the translational component of the core shroud is used. The input motions are obtained from a seismic analysis of a coupled internals and core model which has a much less detailed representation of the core.

The reactor vessel motions are used to excite the coupled internals and core model. The analysis of the coupled internals and core model generates the core plate motions which are amplified by a factor of more than 3 from the reactor vessel motions. The ZPAs of FAP in the east-west direction are 1.401g and 3.201g for OBE and SSE, respectively, and the

corresponding values for CSP are 0.475g and 1.298g (Table 6). The ZPA ratios of OBE to SSE for FAP are 62.7 % and 43.8 % in the north-south and east-west directions, respectively.

3.2.2. Dynamic Response

The responses of the fuel assemblies to the excitations were obtained using the integration of equations of motion by the Runge-Kutta-Gill method for first-order differential equations. The integration time step was determined based on the impact pulse which is typically estimated to be 10 milliseconds for the seismic excitation. The number of steps per pulse will be $(10\times10^{-3})/(2\times10^{-4})=50$ for the constant time step of 2×10^{-4} second, which is large enough for this kind of analysis. In this case, the maximum frequency range encompassed is $[2\pi(20)(2\times10^{-4})]^{-1}=39.8$Hz because time step is almost equal to (1/20)×(minimum period). The 39.8Hz is wide enough to cover the fuel assembly frequencies because fuel assembly responds to the seismic excitation by moving back and forth approximately at the first mode frequency of 1Hz.

3.3. Results and Discussion

The result of the core analysis consists of peak spacer grid impact loads, fuel assembly moments, shears and deflected shapes. The impact loads are used to evaluate the structural integrity of spacer grids. The deflected shapes which correspond to peak loading conditions—peak displacement, peak shear and peak moment—are used to calculate stresses using a detailed static model of the fuel assembly. The deflected shapes indicated that the fuel assemblies respond to the seismic excitation by moving back and forth across the core at approximately their first mode natural frequencies [15]. The maximum deflection which is found in the middle of the fuel assembly height should be small enough to guarantee a control element assembly insertion [18].

The spacer grid impact loads and the fuel assembly responses are shown in Table 10. The square root of the sum of the squares (SRSS) of one-sided impact are 1935 lbs and 3826 lbs for OBE and SSE, respectively. The OBE impact is almost half of SSE impact. For the through-grid impacts, the SRSS values are 1303 lbs and 2740 lbs for OBE and SSE, respectively. The ratio of OBE to SSE is 48%. For the axial response of fuel assembly, the axial force of fuel rods is 278.5 lbs and 506.2 lbs for OBE and SSE, respectively (Table 11). The response ratio of OBE/SSE ranges in 48 % to 55% for the fuel rods, end fittings and guide tubes. For both directions the response ratio is almost the same as the ratio of input motions. This indicates that the non-linearity of the fuel assembly response is not significant.

Table 10. Horizontal Response Summary of Fuel Assembly

Response	OBE		SSE	
	N-S	E-W	N-S	E-W
Spacer grid[1]				
One-sided impact(lbs)	1455	1275	2606	2801
Through-grid impact(lbs)	948	894	2091	1771
Fuel assembly				
Deflection(inch)	1.210	1.160	1.505	1.596
Shear(lbs)	164	199	298	394
Moment(lb-inch)	3566	3923	5934	7560

[1] Allowables of one-sided and through-grid impacts for UCN 3&4 fuel assembly are 4413 and 3396 lbs, respectively.

Table 11. Vertical Response Summary of Fuel Assembly

Axial force(lbs)	OBE	SSE	Ratio(%)[1]
Fuel rods	278.5	506.2	55.0
UEF	1.1	2.3	47.8
LEF	306.8	556.5	55.1
Guide tubes	24.9	45.2	55.1

[1] OBE/SSE

4. Concluding Remark

Dynamic analyses of the coupled internals and core for UCN 3 and 4 are performed for the seismic excitations. The response relations between OBE and SSE and their response characteristics are investigated for the OBE elimination of the future nuclear power plant design. The comparison of response loads show that upper flanges of UGS and CSB are the most critical components for OBE loadings and further evaluations for the calculation of stress intensities are necessary to ensure adequate design considerations due to OBE elimination. Also, discussed in this paper are the fuel assembly SSE loads and they are compared to OBE loads. The fuel assembly responses are found to be insignificant for the OBE elimination because the response ratio of OBE to SSE is almost the same as that of input motions.

References

1. ASME, ASME Boiler and Pressure Vessel Code, Sec.III, Rules for Construction of Nuclear Power Plant Components, American Society of Mechanical Engineers, (1989)
2. USNRC, Stress Limits for ASME Class 1, 2, and 3 Components and Component Supports of Safety-Related Systems and Class CS Core Support Structures under Specified Service Loading Combinations, Standard Review Plan Section 3.9.3 Appendix A, Rev.1, US Nuclear Regulatory Commission, April (1984)
3. USNRC, Reactor Site Criteria : Appendix A, Seismic and Geologic Siting Criteria for Nuclear Power Plants, 10 CFR Part 100, US Nuclear Regulatory Commission, (1977)
4. ASME, ASME Boiler and Pressure Vessel Code, Sec.XI, Rules for Inservice Inspection of Nuclear Power Plant Components, American Society of Mechanical Engineers, (1989)
5. USNRC, Evaluation of Potential for Pipe Breaks, NUREG-1061, Vol.3, US Nuclear Regulatory Commission, November (1984)
6. USNRC, Licensing of Production and Utilization Facilities : Appendix A, General Design Criteria for Nuclear Power Plants, 10 CFR Part 50, US Nuclear Regulatory Commission, (1976)
7. ABB-CE, "ASME Design Report for Yonggwang Nuclear Power Plant Unit 3−Core Support Structures," 10287-ME-AR-240-00, ABB Combustion Engineering, September (1993)
8. CE, "Evaluation of Reactor Core Support Structures for Arizona Nuclear Power Project Palo Verde Unit 1," 14273-MD-001, Combustion Engineering, Inc., March (1981)
9. USNRC, "Evolutionary Light Water Reactor Certification Issues and Their Relationship to Current Regulatory Requirements," SECY-90-016, US Nuclear Regulatory Commission, January 12, (1990)
10. USNRC, "Policy, Technical, and Licensing Issues Pertaining to Evolutionary and Advanced Light Water Reactor Designs," SECY-93-087, US Nuclear Regulatory Commission, April 2, (1993)
11. Jhung, M.J., *et al.*, "Optimal Design of Control Element Assembly Shroud," *Proceedings of the Fifth International ANSYS Conference*, Vol.3, pp.14.11-14.21, Pittsburgh, May (1991)
12. Jhung, M.J., Choi, S. and Song, H.G., "Analytical Study on the Vibration Characteristics of Control Element Assembly Shroud," *Proceedings of the International Conference on Structural Dynamic Modelling*, pp.69-78, Milton Keynes, UK, July (1993)
13. Jhung, M.J. and Choi, S., "Experimental Study

on the Vibration Characteristics of Control Element Assembly Shroud," *Proceedings of the International Conference on Vibration Engineering*, pp.465-470, Beijing, China, June (1994)

14. Gabrielson, V.K., "SHOCK－A Computer Code for Solving Lumped-Mass Dynamic Systems," Technical Report SCL-DR-65-34, Sandia Laboratories, Livermore, CA, January (1966)
15. Jhung, M.J. and Hwang, W.G., "Seismic Behavior of Fuel Assembly for Pressurized Water Reactor," *Structural Engineering and Mechanics*, Vol.2, No.2, pp.157-171, (1994)
16. Stokes, F.E. and King, R.A., "PWR Fuel Assembly Dynamic Characteristics," *Proceedings of the International Conference on Vibration in Nuclear Plant*, British Nuclear Energy Society, Keswick, UK, (1978)
17. Jhung, M.J., Song, H.G. and Park, K.B., "Dynamic Characteristics of Spacer Grid Impact Loads for SSE," *Journal of the Korean Nuclear Society*, Vol.24, No.2, pp.111-120, (1992)
18. Jhung, M.J., Song, H.G. and Park, K.B., "Evaluation of Control Element Assembly Insertion in the Reactor Internals under Seismic Excitations," *Proceedings of the 4th East Asia－Pacific Conference on Structural Engineering and Construction*, Vol.III, pp.1783～788, Seoul, September (1993)